CNPq

CBPF- CENTRO BRASILEIRO DE PESQUISAS FÍSICAS

Notas de Física

CBPF-NF-011/92

GEOMETRIC EFFICIENCY CALCULATIONS FOR SSTD IN RADON MEASUREMENTS

by

Lelé R. GIL, Alfredo MARQUES and Alice RIVERA

ABSTRACT

Geometric efficiencies for SSTD cut into rectangular pieces are calculated by simulation technique. The procedure involves introducing a sampling volume that depends on α-ray ranges in air which has to be used in converting observed number of tracks into activity concentrations. A quick procedure for computing ranges in air at different meteorological conditions is also included.

Key-words: SSTD; Geometric efficiency; Radon.

1 INTRODUCTION

A general analitic solution for geometric efficiency calculation is easily formulated [1] and although the procedure may be used with any geometry,for rectangular shape detectors it becomes lengthy, as multiple numerical integrations are involved, besides requiring some mathematical skill in handling contours of integration numerically . We found it convenient to try an alternate solution by using simulation techniques: instead of the multiple integration problem we solved the equivalent one of determining the fraction of all α -rays,emitted at random angles and distances to detector's surface, that hit it. Owing to their finite ranges, α- rays emitted at positions external to a certain critical volume around the detector can never reach its surface and their inclusion in calculations, both in simulation and multiple integration procedures, will but lengthen the computing time.That volume, in short,the "sampling volume", is here defined as the region of space outside which emitted α-rays are forbidden to reach detector's surface on account of geometrical limitations related to their finite ranges. The size of that volume, depending upon α-ray ranges in air, will vary for different members of the radioactive family; this situation has implications when converting α-ray counts to specific activities and in assessing quantities related to radioactive equilibrium when α-ray groups are not separated, as it is the case usually with SSTD. Since α -ranges are essential to define the sampling volume we also give a range-energy procedure to determine α-ray ranges in air, that may be used under different meteorological conditions as it is required in Radon measurements underground,at sites high up sea level and to cover

seasonal and/or latitude temperature variations.

2 EFFICIENCY CALCULATIONS

Calculations were restricted to squared and rectangular shape detector , as it happens usually with SSTD; for ionization chambers, particularly solid state ones,cylindrical geometry is dominant and efficiencies are obtained by multiple integration as indicated in ref[1]. The questions related to the sampling volume,however, apply equally. For a rectangular shape detector surface with half- sides a,b,the sampling volume for α-rays with range R_α in air is the volume of a right prism whose basis is a rectangle with half- sides $a+R_\alpha$, $b+R_\alpha$ and height R_α (for incidence on just one of the faces of the detector).Trajectories of α-rays emitted at points outside that volume will never intersect detector's surface, supposed to occupy the central region of the rectangular basis.In terms of a coordinate system with center at the detector's center, occupying the plane z=0, only α-rays emitted at points X,Y,Z such as $|X|\leq a, |Y|\leq b, Z\leq R_\alpha$ will be accepted as a countable event (as mentioned before, access to the detector is through one of its faces).Coordinates X,Y,Z of points within the limits of the sampling volume where α-ray emission takes place, are obtained by means of a pseudo random number generator in a computer; next,emission polar angles are chosen randomly over the sphere and the coordinates x',y' of the intersection with the plane z=0 are obtained;when the intersection belongs to detector's surface, and also when the length of trajectory from emission point to that of intersection is not greater than R_α ,the event is

counted as a success. The ratio of successes to the total number of events tried tends to the efficiency of the detector as the number of simulations becomes large.The actual number of simulations was, in each case, determined by a compromise between keeping computing time under sizeable limits and statistical precision. Figs. 1-3 show details of the simulation procedure useful to appreciate geometrical features.Fig. 1 displays normalized coordinates, $X/(a+R_\alpha)$,$Y/(b+R_\alpha)$, of emission positions of accepted α-rays,*i.e.*,those that hit the detector with track length in air not greater than the range; Fig. 2 shows the frequency histogram of Z/R_α also for accepted α-rays; Fig. 3 displays the scatter plot of the impact points in detector's surface.All figures refer to a rectangular shape detector with dimensions 2 cm x 3 cm and R_α = 10 cm. Although impacts in detector's surface are evenly distributed, emission positions for α-rays are not uniform in sampling volume.

3 RANGES IN AIR

Range of α-rays in air under different meteorological conditions were computed by combining first principle calculations for H_2,O_2 and N_2 by BICHSEL and PORTER [2] with empirical results for those gases by ZIEGLER and CHU [3].

Following the usual procedure,ranges are calculated by

$$R = \int_{E_o}^{E_L} dE/S \qquad (1)$$

where S is the stopping power.Energy transfer processes, in the course of degrading particle's kinetic energy from the initial value E_o down to rest, follow different regimes and no unique expression exists for S, covering all of them. By limiting the integration (1) to energies $E_L \approx$ 500 keV one looses but an interval of trajectory of length negligeable as compared to the path length from E_o to E_L , as long as $E_L \ll E_o$. Since BICHSEL's first principle calculations do not work down to that limit, for H_2,$N_2$and O_2 , we found it convenient to extend them down to E_L by completing the tabulated values with ZIEGLER's semi-empirical data; the two sets of data are found to agree to within 5% [2].

Least square curves were fitted to the extended data in each case leading to the following results: i)$S(O_2)=1777.037E_\alpha^{-0.550}$; ii)$S(N_2)=1962.574E_\alpha^{-0.584}$; iii)$S(H_2)=7257.530E_\alpha^{-0.731}$, where E_α is the energy in MeV and S is in mg/cm^2.Those expressions will represent the extended data to within 5% error over the major part of the interval E < 10 MeV but the fit becomes worse near the low energy end where deviations raise to the 15% level; we assume this circumstance to be perfectly tolerable in view of observation and other errors.

The stopping power for mixture of gases and for water vapour were obtained by following the usual additivity rule [4]; in particular, to find the stopping power for humid air we used: $S(\text{humid air})=[(\rho_{HD}-\rho_{DY})S(H_2O)+\rho_{DY}S(\text{dry air})]/\rho_{DY}$ where ρ_{HD} and ρ_{DY} are densities of humid and dry air respectively.Expressions for those densities are easily obtained from simple considerations of perfect gases thermodynamics or taken directly from tabulations [5]. Following the same rule the stopping power for dry air is obtained from $0.21\ S(O_2) + 0.79\ S(N_2)$ and the stopping power for water

vapour from $[S(H_2)/2+4S(O_2)]/9$. Those parameters allow for the calculation of S(humid air) which is then taken to (1) for numerical integration. It happens, after calculations, that ranges are insensitive to the degree of relative humidity, except for extreme cases of pressure and temperature, and that the dependence with atmospheric pressure is rather mild. Table I shows results for the relevant components of Rn family at atmospheric pressure of 760 mm and selected temperatures.

4 RESULTS AND DISCUSSION

In spite of the impact distribution to be uniform on detector's surface, as shown in Fig.3 , emission positions do not fill uniformily the sampling volume, as seen in Figs.1 and 2. There is a neat tendency for concentration of events in the immediate neighborhood of z-axis and a preference for short distances to detector's surface. Both have to do with variations of solid angle as seen from different space positions in the sampling volume.

Fig.5 shows the geometric efficiency per unit area as a function of the length of side for squared shape detectors. That behaviour is also a consequence of the uneven character of the space distribution of emitting centers and calls for a word of warning about the common practice of reducing data observed in small regions all over a large area detector to an average per unit area; data coming from detectors with different areas will be not comparable.

When converting the number of tracks registered during the

experiment into activity concentration one must take into account the sizes of the sampling volumes for each α- range. Although different groups of α-rays are not separated in SSTD, the observations may yet be useful in connexion with situations of radioactive equilibrium if one calculates the efficiency by:

$$E = f_0 E_0 + f_1 E_1 + f_2 E_2 \qquad (2)$$

where: $f_0 = [1+\lambda_0 v_1/\lambda_1 v_0+\lambda_0 v_2/\lambda_2 v_0]^{-1}$

$f_1 = [1+\lambda_1 v_2/\lambda_2 v_1+\lambda_1 v_0/\lambda_0 v_1]^{-1}$; $f_2=[1+\lambda_2 v_1/\lambda_1 v_2+\lambda_2 v_0/\lambda_0 v_2]^{-1}$

where it is supposed that there are no more than three α-emitters in equilibrium : λ_0, λ_1, λ_2 are the disintegration constants and v_0, v_1, v_2 the sampling volumes, E_0, E_1, E_2, the detection efficiences for each member; the index "o" stands for the head of the family.

Table II shows the values of sampling volumes and average geometric efficiencies for detection of α-rays from relevant members of Rn family in air at 760 mm and at the indicated temperatures, for detectors of different sizes, squared and rectangular shapes; errors quoted are only statistical, related to fluctuations in random numbers generation.

Finally we notice that the effect of casting a "shadow" in detector's surface by objects occupying even partially the sampling volume might have been observed by BIGAZZI,HADLER and PAULO [6]; this circumstance may call for judicious interpretation of "plate out" effects when the distance from detector to the wall is shorter than the α-ray range.

CAPTIONS FOR FIGURES

FIG.1 - Distribution of Normalized Projections of Emission Positions on Detector's Plane for α-Rays in Samp[ling Volume that hit its Surface with Pathlength not greater than R ; a=1cm; b=1.5cm; R_α=10cm.

FIG.2 - Frequency Distribution of Distances to Detector's Plane of Emission Positions for successful α-Rays.

FIG.3 - Distribution of Normalized Impact Positions at Detector's Surface;a=1cm;b=1.5cm; R_α=10cm.

FIG.4 - Scatter plot of normalized coordinates of emission positions for accepted α-rays.

FIG.5 - Efficiency per Unit Area as a Function of Length of Side for Squared Shape Detector's.

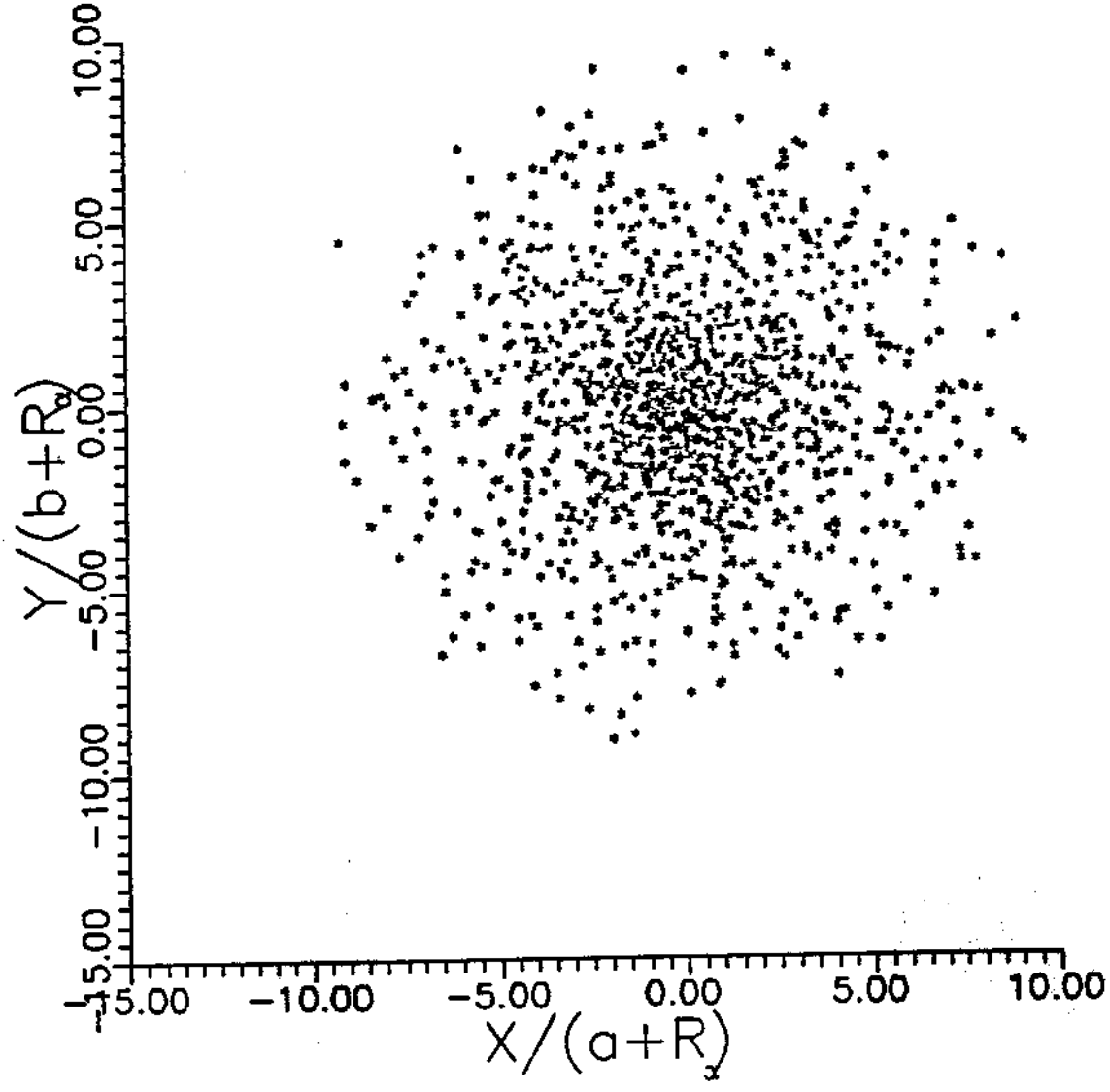

FIG. 1

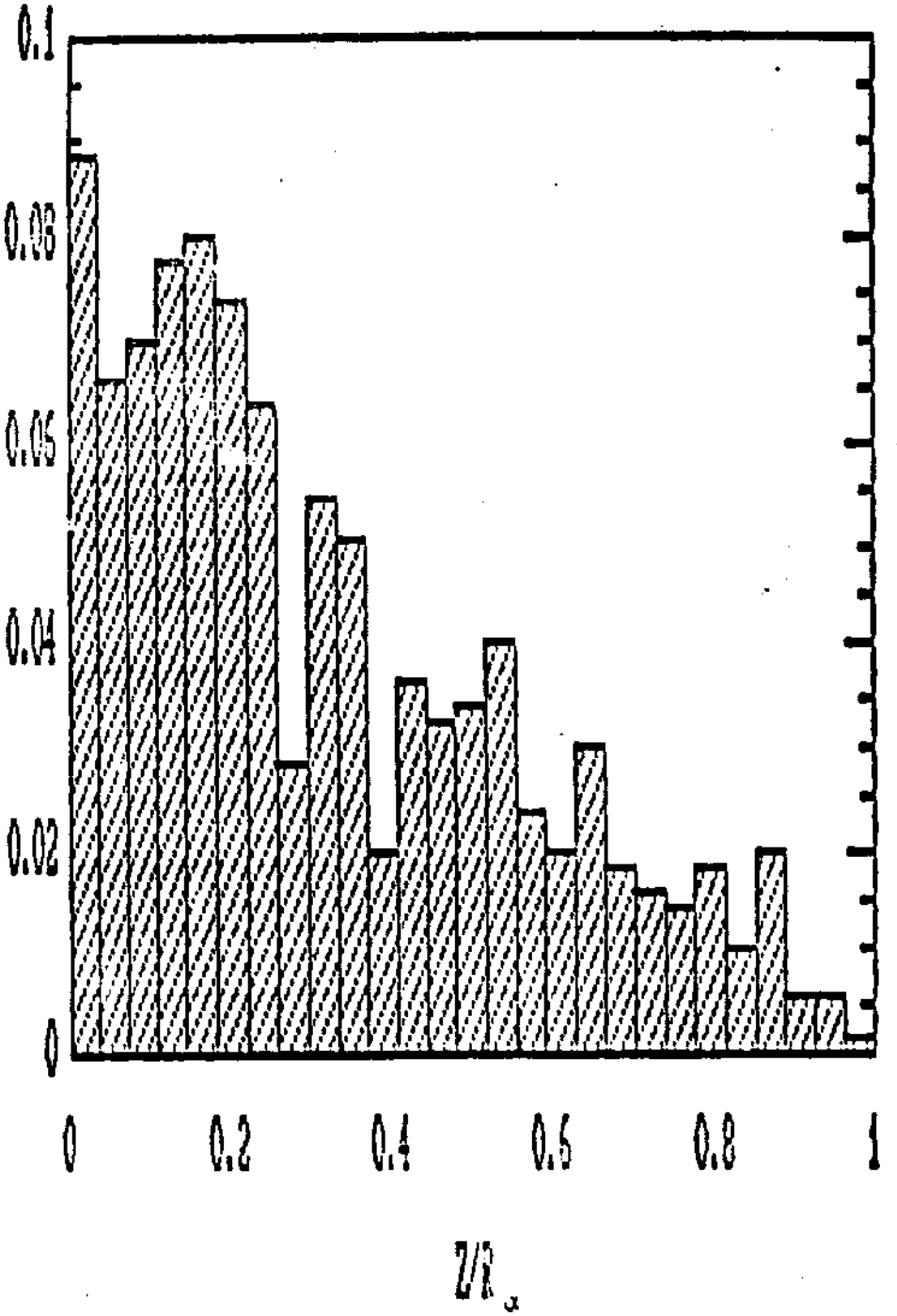

FIG. 2

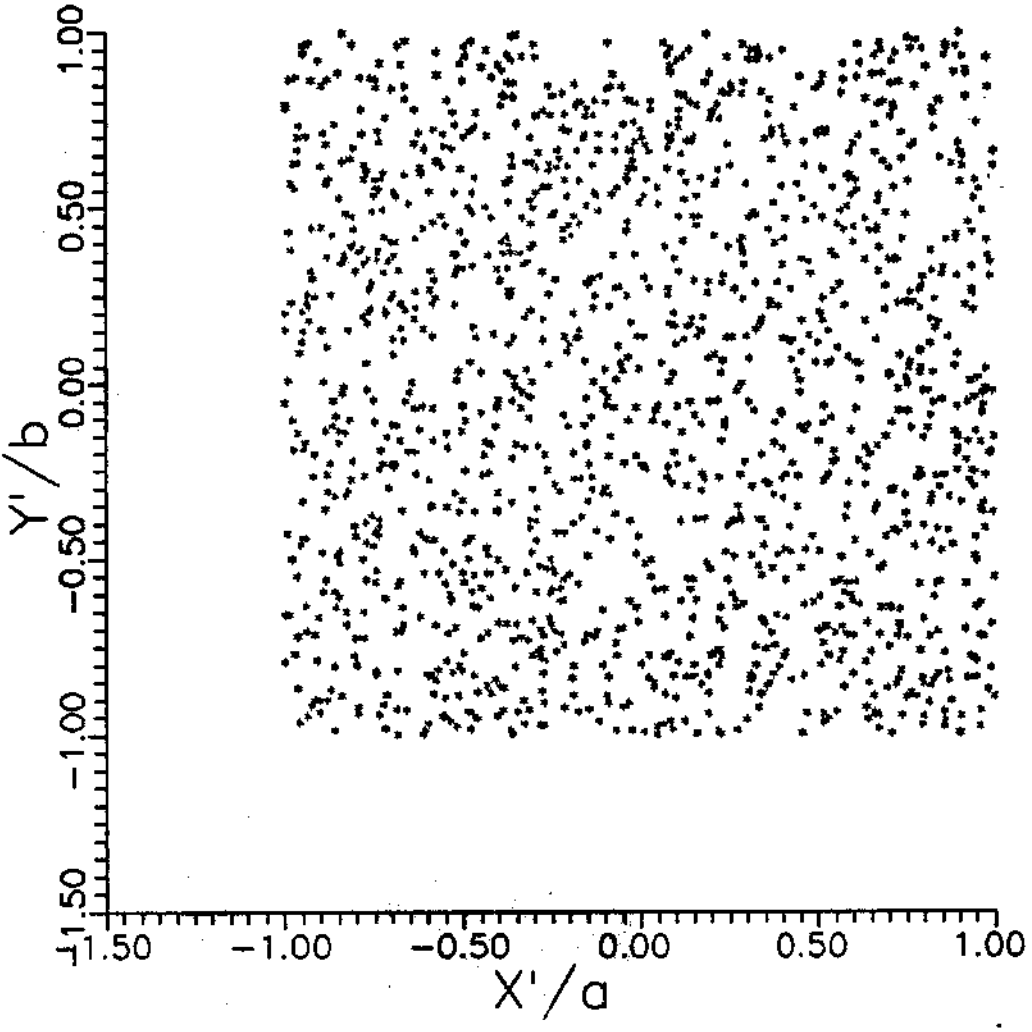

FIG.3

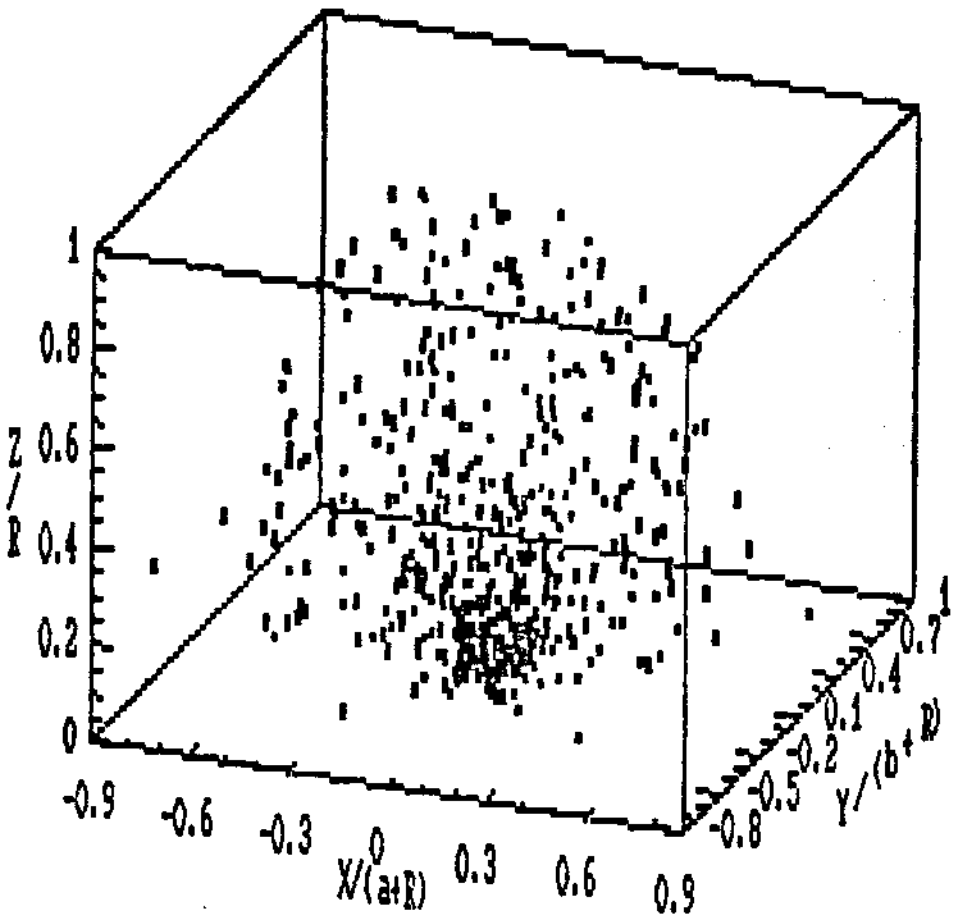

FIG. 4

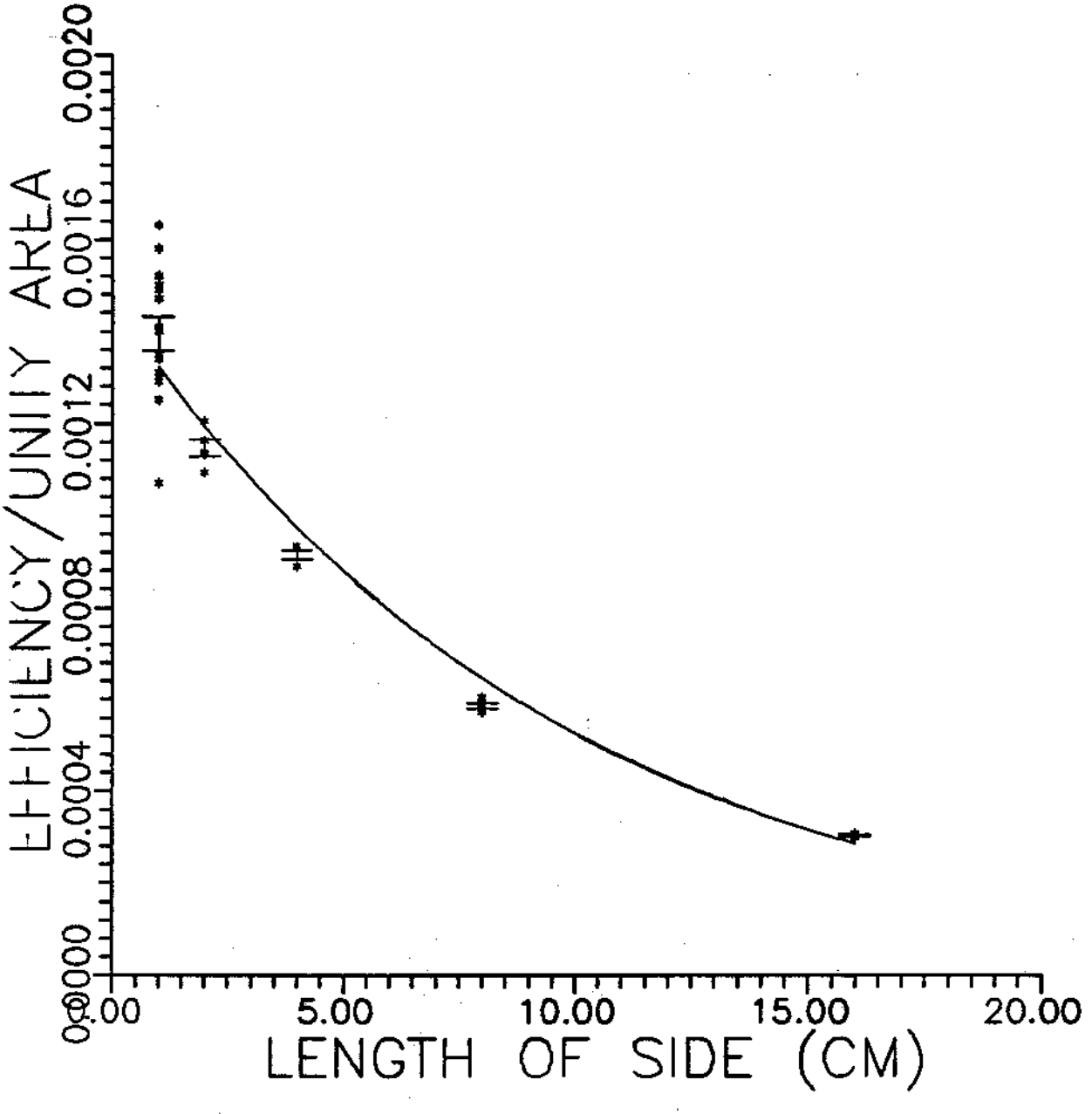
EFFICIENCY/UNIIY AREA
0.0000
0.0004
0.0008
0.0012
0.0016
0.0020
0.00
5.00
10.00
15.00
20.00
LENGTH OF SIDE (CM)

FIG. 5

TABLE I

RANGES AND SAMPLING VOLUMES FOR DIFFERENT DETECTOR DIMENSIONS
p=760 mm

T(C)	α-Emitter	Range (cm)	Sampling Volume ($cm^3 x 10^{-3}$)			
			1x1	3x3	5x5	3x5
0	Rn	5.64	0.212	0.287	0.374	0.327
	RaA	6.34	0.297	0.389	0.495	0.439
	RaC'	9.51	0.953	1.153	1.372	1.257
20	Rn	6.09	0.264	0.357	0.449	0.397
	RaA	6.88	0.374	0.483	0.605	0.541
	RaC'	10.32	1.208	1.442	1.696	1.564
40	Rn	6.67	0.343	0.445	0.561	0.500
	RaA	7.55	0.489	0.618	0.762	0.687
	RaC'	11.32	1.581	1.860	2.162	2.006

TABLE II

EFFICIENCY ($x10^3$) FOR DIFFERENT DETECTOR DIMENSIONS
p=760 mm

Dm (cm)	T(^{0}C) α-Emitter	0	20	40
1x1	Rn	1.636±0.131	1.418±0.104	1.044±0.095
	RaA	1.328±0.123	1.112±0.070	1.086±0.079
	RaC'	0.628±0.038	0.542±0.025	0.430±0.074
3x3	Rn	11.21 ±0.043	9.800±0.172	8.320±0.129
	RaA	9.112±0.298	7.760±0.145	6.858±0.409
	RaC'	4.836±0.105	3.892±0.141	3.276±0.206
5x5	Rn	23.68 ±0.39	21.07 ±0.49	18.14 ±0.23
	RaA	19.80 ±0.33	17.73 ±0.19	15.46 ±0.29
	RaC'	10.71 ±0.15	9.352±0.285	8.166±0.182
3x5	Rn	16.44 ±0.19	14.34 ±0.16	12.46 ±0.17
	RaA	13.48 ±0.36	11.98 ±0.33	10.15 ±0.38
	RaC'	7.172±0.050	6.096±0.184	5.344±0.076

REFERENCES

[1] R.L.FLEISCHER and A.MOGRO-CAMPERO, J.Geophys.Res. **83** 1978,3539

[2] H.BICHSEL and L.E.PORTER, Phys.Rev. **A25** (1982),2499

[3] J.F.ZIEGLER and W.K.CHU, At.Data and Nucl.Data Tables, **13** 1974,463

[4] M.J.BERGER and S.M.SELTZER, Stopping Powers and Ranges of Electrons and Positrons, 2nd Ed.NBSIR 82-2550A 1983

[5] HANDBOOK OF CHEMISTRY AND PHYSICS, Charles D.Hodgman 32nd Ed., Chemical Rubber Publishing Co. 1950

[6] G.BIGAZZI, J.C.HADLER and S.R.PAULO, Nucl.Instr. and Meth. **A280** 1989,506